Feasibility of Detecting Aflatoxin B_1 on Inoculated Maize Kernels Surface using Vis/NIR Hyperspectral Imaging

Wei Wang, Gerald W. Heitschmidt, William R. Windham, Peggy Feldner, Xinzhi Ni, and Xuan Chu

Abstract: The feasibility of using a visible/near-infrared hyperspectral imaging system with a wavelength range between 400 and 1000 nm to detect and differentiate different levels of aflatoxin B_1 (AFB_1) artificially titrated on maize kernel surface was examined. To reduce the color effects of maize kernels, image analysis was limited to a subset of original spectra (600 to 1000 nm). Residual staining from the AFB_1 on the kernels surface was selected as regions of interest for analysis. Principal components analysis (PCA) was applied to reduce the dimensionality of hyperspectral image data, and then a stepwise factorial discriminant analysis (FDA) was performed on latent PCA variables. The results indicated that discriminant factors F_2 can be used to separate control samples from all of the other groups of kernels with AFB_1 inoculated, whereas the discriminant factors F_1 can be used to identify maize kernels with levels of AFB_1 as low as 10 ppb. An overall classification accuracy of 98% was achieved. Finally, the peaks of β coefficients of the discrimination factors F_1 and F_2 were analyzed and several key wavelengths identified for differentiating maize kernels with and without AFB_1, as well as those with differing levels of AFB_1 inoculation. Results indicated that Vis/NIR hyperspectral imaging technology combined with the PCA–FDA was a practical method to detect and differentiate different levels of AFB_1 artificially inoculated on the maize kernels surface. However, indicated the potential to detect and differentiate naturally occurring toxins in maize kernel.

Keywords: aflatoxin B_1 (AFB_1), factorial discriminant analysis (FDA), hyperspectral imaging, maize, principal components analysis (PCA)

Practical Application: This work can lay a foundation for future development of practical grain sorting equipment just after harvest, and for further research on detection of field maize kernels with natural aflatoxin infection.

Introduction

Maize is one of the major food and cash crops grown worldwide. However, maize kernels are subject to infection by a variety of toxigenic fungi (Abbas and others 2006). The fungi *Aspergillus parasiticus* and *Aspergillus flavus* produce toxic and carcinogenic secondary metabolites called aflatoxins (Wright and others 2000). The Intl. Agency for Research on Cancer (IARC) has classified aflatoxin B_1 (AFB_1), AFB_2, AFG_1, and AFG_2 as group 1 carcinogens (IARC 2002; Manetta 2011). Among this group of toxins, AFB_1 was found to be one of the most potent environmental carcinogens. The intake of AFB_1 over a long period of time, even at very low concentration, may be highly dangerous (Piermarini and others 2009). Consequently, aflatoxin has long been monitored by the United States Food and Drug Administration (USFDA), and a level of 20 ppb has been set as the limit for maize contamination with aflatoxin (Abbas and others 2006). The early detection of toxigenic fungi directly on maize kernels can be useful to prevent the intake of these contaminated materials into the food chain (Del Fiore and others 2010).

Conventional analytical method used to detect and quantify the toxicity in grain and feeds include thin layer chromatography (Samarajeewa and others 1991), gas chromatography, and high performance liquid chromatography (HPLC; McDanell and others 1988; Herzallah 2009). There are also some other methodologies including immunosorbent assay (Waśkiewicz and others 2012), molecular identification techniques (Borman and others 2008), and fluorescence (Fernández-Ibañez and others 2009; Gorran and others 2013). Although these methods have many merits such as accuracy, selectivity, very low limit of detection or rapidity, most of these methods are generally expensive, difficult, and introduce unfriendly chemicals (Christensen and others 2008). For detection of mycotoxins at grain processing plants, an objective, rapid, and nondestructive method is needed (Fernández-Ibañez and others 2009).

In the past few decades, studies have been focused largely on near infrared (NIR) spectroscopy, a nondestructive, simple, rapid, and inexpensive methods for the screening of fungal contamination and toxins on cereals. For example, Dowell and others (1999) used NIR spectroscopy to predict *Fusarium* head blight (FHB) disease, vomitoxin, and ergosterol in single wheat kernels. Wang and others (2004) classified fungal-damaged soybean seeds, Berardo and others (2005) detected kernel rots and mycotoxins in maize. Pearson and others (2001) used transmittance and reflectance spectroscopy for detecting aflatoxin

MS 20131726 Submitted 11/20/2013, Accepted 10/29/2014. *Authors Wang and Chu are with College of Engineering, China Agricultural Univ., No. 17 Tsinghua East Rd., Beijing, 100083, China. Authors Heitschmidt, Windham and Feldner are with Quality & Safety Assessment Research Unit, Richard B. Russell Research Center, USDA-ARS, 950 College Station Rd. Athens, GA, 30605, U.S.A. Authors Ni are with Crop Genetics and Breeding Research Unit-USDA-ARS, 2747 Davis Road, Tifton, GA, 31793, U.S.A. Direct inquiries to author Wang (E-mail: playerwxw@cau.edu.cn)*

doi: 10.1111/1750-3841.12728

Journal of Food Science A Publication of the Institute of Food Technologists

in single corn kernels. Delwiche and Gaines (2005) also developed 2-wavelength models in the visible (Vis), NIR, and the hybrid region for sorting of *fusarium*-damaged wheat, achieving at least 86% classification accuracy. Tripathi and Mishra (2009) indicated that the most significant bands related to fungal infection were around 870 to 1200 nm corresponding to NH in most amino acids and aromatic rings. Peiris and others (2009) concluded that differences in peak height attributed to changes in the levels of grain food reserves such as starches, proteins, and lipids and other structural compounds, and positions shifts may arise from other NIR active compounds, such as deoxynivalenol.

Conventional NIR spectroscopic techniques provide an average spectrum of the targeted sample without any spatial information. When measuring bulk-samples, results do not indicate whether the average toxin values resulted from a single highly infected kernel, a few modestly infected kernels, or several kernels infected at a low level (Dowell and others 1999). For this reason, detection with a point-source instrument can become problematic (Polder and others 2005). However, hyperspectral imaging allows characterization of both the spectral (spectroscopic component) and spatial properties (imaging component) of a given sample because each pixel in a hyperspectral image contains the full spectral response across a range of wavelengths, typically, UV-Visible, Vis/NIR, SWIR, or thermal IR (Del Fiore and others 2010). Thus, hyperspectral imaging technology is an ideal information tool to detect the presence of fungi or mycotoxins and determine their distribution on maize samples. Singh and others (2010, 2012) and Shahin and Symons (2011) used hyperspectral imaging method to detect midge-damaged wheat kernels. Delwiche and Kim (2000) showed the application of the hyperspectral reflectance imaging to separate healthy wheat kernels from those damaged by FHB. Williams and others (2012) presented a hyperspectral imaging method for detection of *Fusarium* in maize kernels. In addition, Polder and others (2005) found the NIR range is much more suitable than the visible range to detect FHB in whole wheat kernels.

Pearson and others (2001) suggested that AFB_1 typically localized at the kernel embryo and can leave little indication of its presence on the kernel surface, therefore it was improbable to detect AFB_1 directly by NIR spectroscopy. Dowell and others (2002) concluded that fumonisin present at the ppm level do not absorb detectable amounts of NIR energy. However, other chemical and optical properties of whole kernels caused by fungi or mycotoxin may be detected with Vis or NIR spectroscopy. Berardo and others (2005) reported that the mold infection and metabolites produced in maize grain and flour by *Fusarium verticilloides* could be quantified using NIR spectroscopy. In addition, Fernández-Ibañez and others (2009) found that when compared with other conventional methods of screening raw maize kernels, NIR spectroscopy proved to be a rapid, low-cost, and effective method to detect aflatoxin presence at 20 ppb.

Given the contrary findings based on naturally occurring fungal metabolites, it was determined that a controlled experiment was needed wherein maize kernels would be inoculated with AFB_1 at various concentrations and compared with a control group that was free of any AFB_1.

Therefore, the aim of this work is to determine the feasibility of using Vis/NIR hyperspectral imaging technology to detect various concentrations of AFB_1 directly applied to the surfaces of maize kernels. Specifically, the objectives of this study were to: (1) measure the spectral response of maize kernels with pure AFB_1 artificially inoculated on the surface and determine any key wavelengths, (2) establish a model to discriminate between clean and contaminated kernels, and discriminate between kernels artificially inoculated with different levels of AFB_1, and (3) explain the key wavelengths used to differentiate clean maize kernels from those with AFB_1 on their surfaces.

Materials and Methods

Sample preparation

A total of 150 Pioneer 3394 maize kernels with roughly the same size, appearance, shape, and weight were used as the samples in this study. All of the kernels belonged to the same pedigree, harvested in 2010, and were kindly provided by the Toxicology and Mycotoxin Research Unit, Russell Research Center, USDA, ARS. Kernels were originally stored in a good condition, and only those healthy, ripe, and shiny ones were selected as the samples. Furthermore, before the experiment, several kernels of the same batch

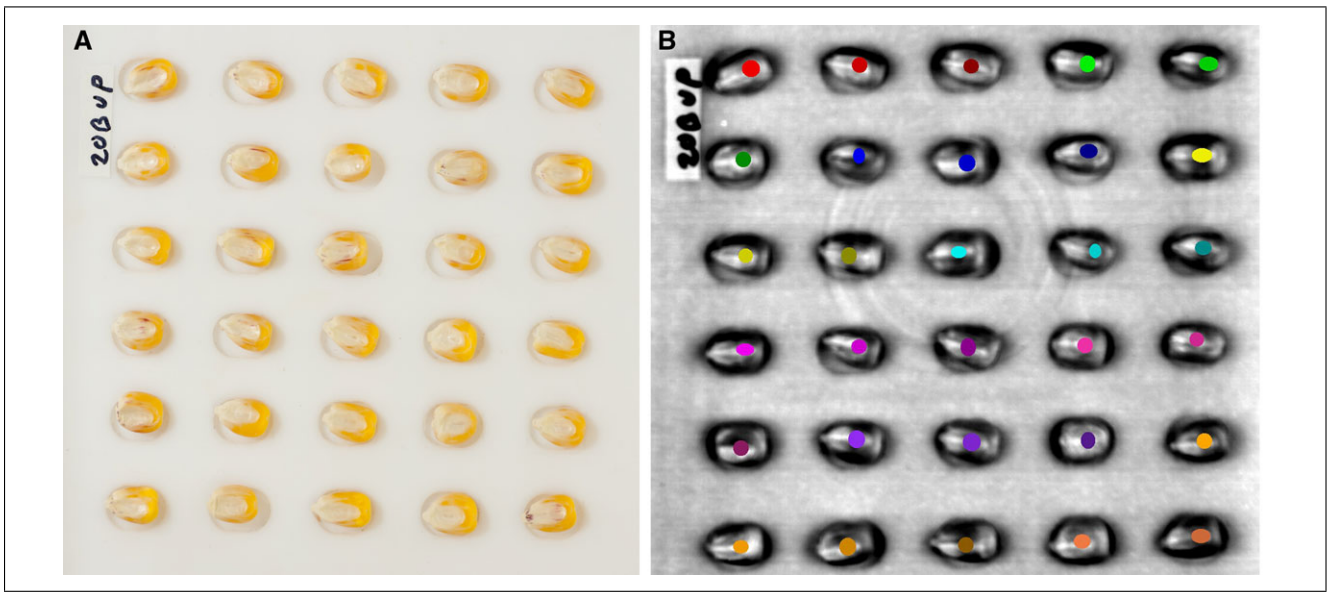

Figure 1–Color photograph and spectral image of maize samples inoculated with 500 ppb AFB_1. (A) Color photographs and (B) selection of ROIs on hyperspectral image.

were randomly selected for testing using HPLC to make sure there were no preexisting natural toxins. By diluting *Aspergillus flavus* aflatoxin (Sigma-Aldrich, 3050 Spruce St., St. Louis, Mo., U.S.A.) with methanol, which was also used to kill any residual mold spores in AFB_1, and according to the average kernel weight 0.33 g, 4 concentrations of stock solutions, that is 10, 20, 100, and 500 ppb, were prepared. For the detailed procedure please refer to Wang and others (2014). Once the solutions were prepared, the kernels were divided into 5 groups. The 1st group consisted of 30 kernels that served as the control group. The control group was treated with methanol alone, whereas the other 4 groups, consisting of 30 kernels each, were inoculated with 10, 20, 100, and 500 ppb AFB_1 solutions, respectively, using a pipette. After inoculation, each group was placed in a chemical hood for approximately 90 min to facilitate drying. Before imaging, kernels from a given group (30 at a time) were placed on a Teflon® sample holder containing 30 shallow, elliptically shaped wells arranged in 6 rows × 5 columns (Figure 1A). As a safety measure, the Teflon holder was placed inside of a special transparent sealed box before imaging (Wang and others 2014).

Hyperspectral Image acquisition and preprocessing

A Vis/NIR hyperspectral imaging system with a wavelength range of 400 to 1000 nm was used for this study. The system included a sCMOS PCO.EDGE camera (PCO-TECH, Romulus, MI, U.S.A.), spectrograph (V10M, Specim, Oulu, Finland), front lens (Distagon T 25 mm f/2.8, Zeiss, Oberkochen, Germany). Indirect lighting was provided by 2 softboxes with 500 W Tungsten–Halogen lamps positioned at approximately 45° angles above and lateral to the samples (SilverDome® nxt: small, Photoflex, Watsonville, Calif., U.S.A.). The hyperspectral imaging system was spectrally calibrated using a series of pencil style calibration lamps and lasers (Wang and others 2014). A 75% Spectralon® reflectance panel was imaged and used for image calibration (SRT-75-050, Labsphere, North Sutton, N.H., U.S.A.).

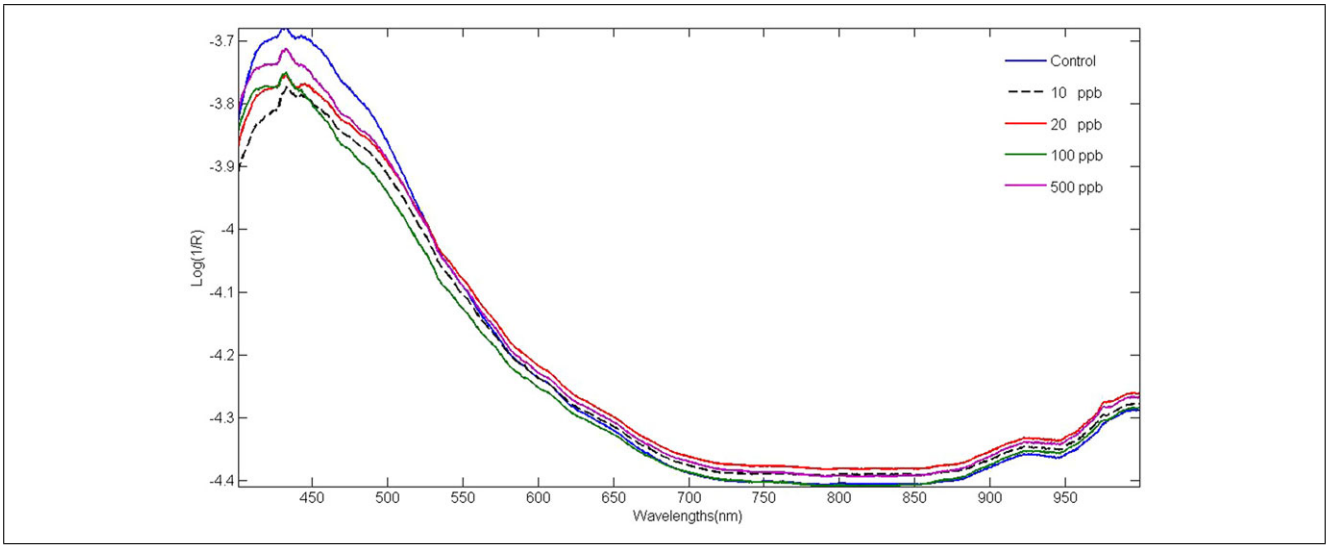

Figure 2–The original average spectra of the 5 groups of maize kernels.

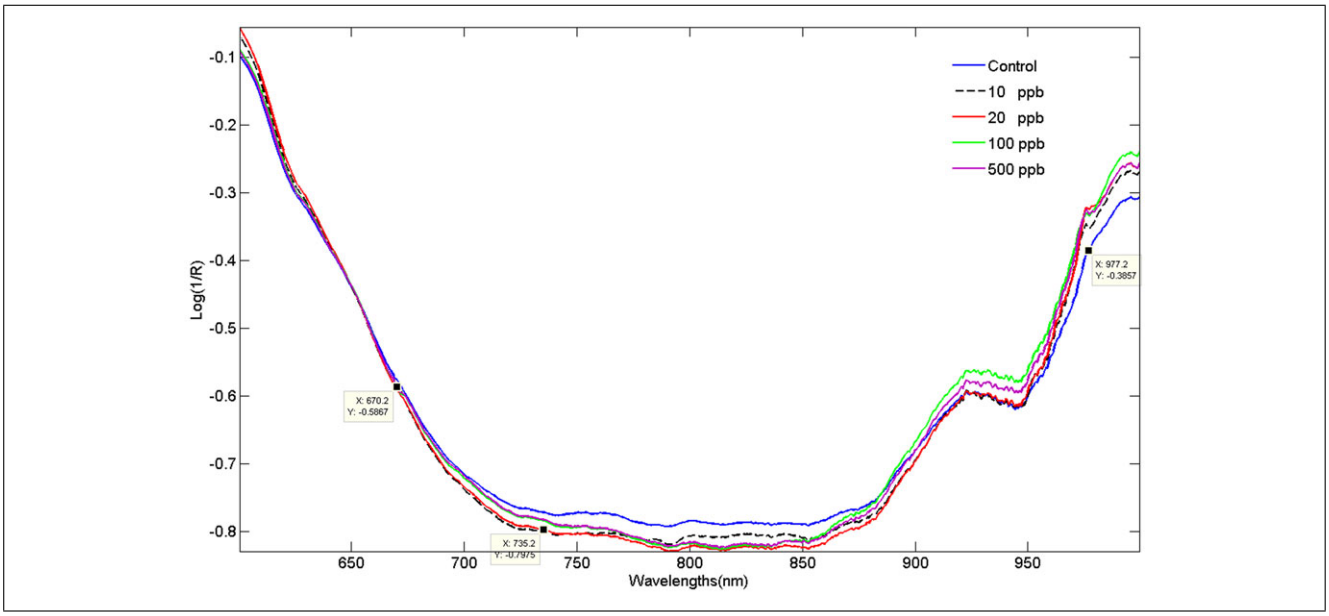

Figure 3–The average subset spectra (600 to 1000 nm) of the 5 groups of maize kernels with SNV corrected.

HyperVisual® software was used for image acquisition and some preprocessing of the imagery (PhiLumina, Gulfport, Miss., U.S.A.). During image acquisition, the samples remained motionless whereas the software controlled the scanning process. HyperVisual was used to spectrally subset the imagery to 400 to 1000 nm and to calibrate it to percent reflectance. Noise inherent to these images was then removed using ENVIs (Exelis Visual Information Solutions, Boulder, Co., U.S.A.) minimum noise fraction (MNF)/inverse MNF processing flow (Wang and others 2014).

Regions of interest (ROIs)

To limit the analysis to those areas on the kernels where AFB_1 was applied, ROIs were created where the methanol or methanol/aflatoxin dilutions had left a visible dry, white stain on the kernel surfaces. Elliptical ROIs of AFB_1-inoculated maize kernels were hand-digitized using ENVI software. A 50-pixel minimum ROI size was targeted for all kernels, however when this was not possible, ROIs contained as many pixels as possible (Figure 1B). The process of ROI creation was the same for both the control and inoculated groups (Wang and others 2014). The mean reflectance from within each ROI was calculated and then transformed to log(1/reflectance) to represent absorption. Saisir software (Version 07/01/2009, France), a free package for chemometrics with MATLAB (The MathWorks, Natick, MA, USA), was used to develop prediction models in this work.

The PCA–stepwise factorial discriminant analysis (FDA) method

The main goal of PCA in this work was to reduce the spectral dimensionality of the hyperspectral imagery, which typically contains highly correlated information in neighboring bands (Williams and Norris 1987). Minimizing data dimensionality was a necessary 1st step for the discriminant technique that followed (Castellano and others 2007; Karoui and others 2011; Wang and others 2014).

In general, discriminant techniques attempt to predict the fit of a statistical unit to *a priori* classes based on assumed values for *p* predictors, which are usually numerical (Lauro and others 2007). The FDA technique assesses new synthetic variables called "discriminant factors," which are linear combinations of selected PCs that allow separation of the center of gravity of the considered groups (Hammami and others 2010).

The stepwise FDA, with the optimization of variable selection as outlined in Roger and others (2002), was adopted in this paper. Instead of selecting the best linear combination using the whole set of variables, as the FDA usually does, the stepwise FDA in this paper was used to predict to which of the 5 groups (control, 10, 20, 100, and 500 ppb group) individual maize kernels belonged (Lin and others 2012; Ivorra and others 2013; Vitale and others 2013). For each group, the 1st two thirds of the 30 samples were attributed to the calibration set and the rest to the validation set. Therefore, in total, the calibration set included 100 samples and the validation set consisted of 50 samples. For each individual sample, its distance from the various centers of gravity of each group was calculated, then the individual sample was assigned to the group with the nearest gravity center (Wang and others 2014).

Results and Discussion

The original spectra and its spectral subset

The original average spectra of the total 150 samples (including all of the maize kernels attributed to calibration and validation set) with the wavelength range between 400 and 1000 nm were plotted in Figure 2. Of the spectra, the prominent changes between different samples appeared mostly within the range between 400 and 600 nm. However, as Fernández-Ibañez and others (2009) indicated, spectral differences in the 400 to 600 nm region are associated with color changes in fungal infected cereal grains. Del Fiore and others (2010) also explained that higher apparent absorbance log(1/*R*) values in the 500 to 600 nm spectral range were caused by the presence of a large amount of carotenoids on the kernels' epicarp. For this reason, it was determined to omit the spectral information caused mainly by color variations in the kernels. Thus, the spectral analysis for this study was limited to the 600 to 1000 nm spectral range.

Furthermore, to get rid of the scattering effects caused by different surface roughness and kernel shape, standard normal variate correction (SNV) was applied to the data. The mean spectra (600 to 1000 nm) with SNV corrected of the 5 groups of maize kernels are shown in Figure 3. Some significant differences in absorption between the 5 groups of maize kernels are evident at wavelengths 670.2, 735.2, and 977.2 nm.

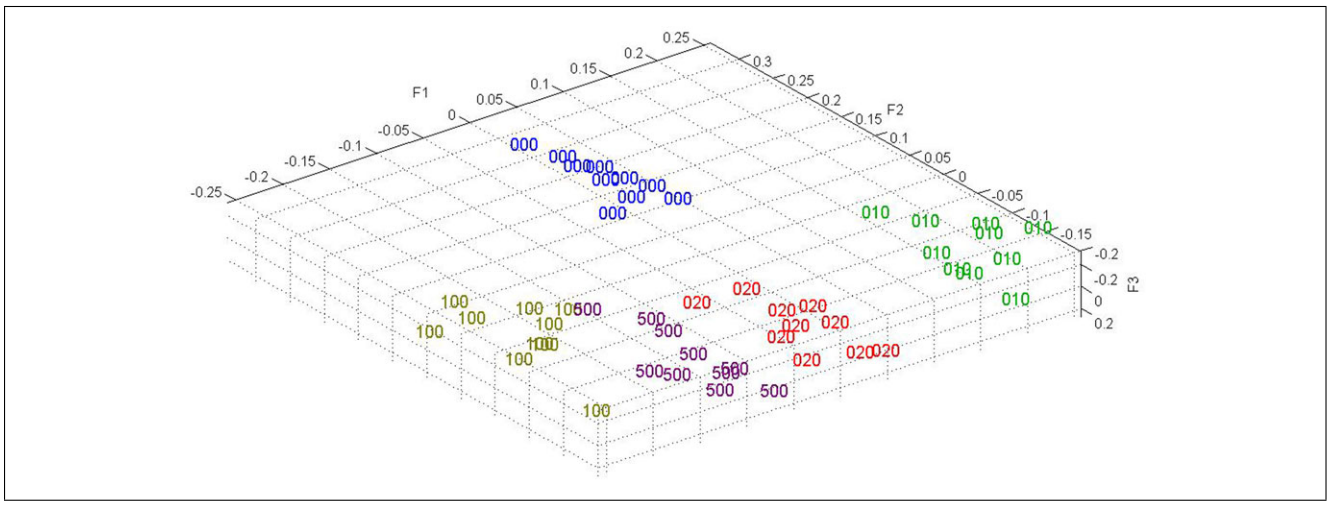

Figure 4–Distribution of validation kernels in the coordinate space constituted by the 1st 3 discriminant factors.

Table 1–Confusion matrix of discriminant results for validation kernels.

	Predicted concentration (ppb)				
Actual concentration (ppb)	**0**	**10**	**20**	**100**	**500**
0	10	0	0	0	0
10	0	10	0	0	0
20	0	0	10	0	0
100	0	0	0	10	0
500	0	0	0	1	9

PCA of maize kernels with AFB_1 inoculated

Results from the PCA analysis indicate the 1st 3 PCs scores (PC_1, PC_2, PC_3) contained 79.4%, 12.9%, and 4.4% of the variance, respectively. Based on these 3 components, the control samples could generally be separated from the contaminated ones. However, it was not possible to delineate one contaminated sample group from another based on the amount of aflatoxin applied. This was true even when considering extreme concentration differences, such as 10 ppb versus 500 ppb. This was unexpected since PCA is generally not considered to be an effective statistical test between or among groups as it makes no prior assumption about the data structure (Serranti and others 2013).

FDA classification results

A stepwise FDA was performed on the 1st 20 PCs, and the maximum number of PCs permitted to enter the FDA model was set to 11 in order to avoid the loss of useful information as much as possible. Based on the results, except that 4 PCs (PC15, PC16, PC18, and PC19) representing 0.0% of the variance of the model were cancelled, the rest 7 PCs, that is, PC2, PC5, PC4, PC3, PC9, PC8, and PC6 representing 12.9%, 0.8%, 1.1%, 4.4%, 0.1%, 0.1%, and 0.7% of the variance of the model respectively, were introduced in that order. It is obvious that all the 7 PCs introduced were within the top 10 PCs. Even so, PC1 was omitted by the FDA classification model even though it typically contains the most variance, perhaps because it was heavily influenced by scattering effects due to kernel shape rather than chemical composition (Manley and others 2012) .

After FDA was applied to the PCA scores, the distribution of validation kernels was plotted using the 1st 3 discriminant factors F_1, F_2, and F_3 (Figure 4). As shown in Figure 4, not only could the control samples be separated from the AFB_1-innoculated ones, but also samples with different concentrations of AFB_1 could be clearly discriminated from each other. The confusion matrix shown in Table 1 revealed that the classification accuracy was 100% for the control samples. Although for the inoculated ones, only one sample was misclassified: a 500 ppb kernel was mistaken as 100 ppb kernel. This lone misclassification was likely due to the spectral similarity between the 2 higher concentrations of toxins (100 and 500 ppb). Thus, an overall classification accuracy of 98% was achieved.

Discussion

Good classification results could also be achieved using fewer factors than the 1st 3. For example, Figure 4 indicated that using just the 1st 2 discriminant factors, F_1 and F_2, would produce essentially the same result as including F_3. Indeed, using F_2 slone would enable clear delineation of the control kernels from the AFB_1-inoculated kernels.

To identify the chemical attributes of the kernels, weighted β coefficient curves of the 2 discriminant factors F_1 and F_2 were plotted (Figure 5). Based on key wavelengths identified by the β coefficients, the corresponding chemical compositions were explained below.

As previously mentioned, discriminant factor F_2 could be used to separate control kernels from all of the other kernel groups (that is, those inoculated with AFB_1). The β coefficient curve of discriminant factor F_2 reveals significant peaks at 670.2, 735.2, 873.7, 918.3, 913.3, 977.2, and 985.8 nm. Among the 7 wavelengths, 6 were associated closely with the kernel color and nutrient substances, such as protein, starch, oil, and cellulose. As indicated by Xing and others (2010), 670 nm is very close to an absorption peak for chlorophyll, which is primarily attributed to the residual pigments within the seed coat. As shown in the table of Foss NIR system, 873.7 nm corresponds to N–H 3rd overtone of protein, 918.3 nm corresponds to C–H 3rd overtone of starch (or Cellulose), 913.3 nm to CH_2 oil, 977.2 and 985.8 nm to O–H 2nd overtone of water. These 6 wavelength peaks were consistent with the typical chemical composition of maize. However, 735.2 nm, which is located in the transition between Vis and NIR, was not readily associated with any particular constituent. Nevertheless, it

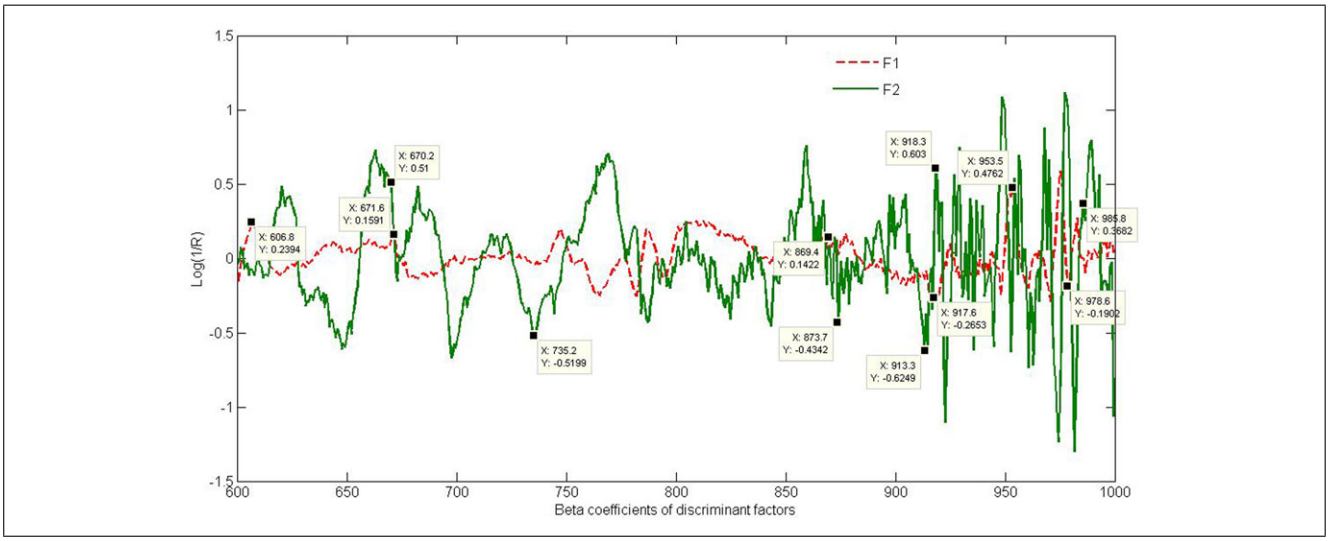

Figure 5–β Coefficient curves of discriminant factors F_1 and F_2.

may be an important wavelength for the delineation of maize kernels containing AFB_1. Pearson and others (2001) effectively used the spectral reflectance ratio 735/1005 nm to distinguish highly contaminated corn kernels (>100 ppb) from those contaminated below 10 ppb, thus demonstrating the potential of 735.2 nm.

Because the discriminant factor F_1 was essential in the differentiation of maize kernels based on their concentrations of AFB_1, the β coefficient peaks of this discriminant factor were also plotted in Figure 5. It is evident from the plot that wavelengths 606.8, 671.6, 869.4, 917.6, 953.5, and 978.6 nm were significant. As indicated by Del Fiore and others (2010), the 870 nm demonstrated the highest loading factor in the 1st PC. Thus, it was considered to be a significant wavelength and was used as input to classify different levels of toxigenic fungi on maize. Also, Singh and others (2010, 2012) found 870 nm to be significant, which corresponded to the CH_3 overtone region. Shahin and Symons (2009) reported 917 nm was an important wavelength for detecting mildew damage on wheat kernels. The wavelength range between 934 and 975 nm has been ascribed to water absorption by Dowell and others (1999), suggesting the 935.5 nm peak found in this research was due to water content. The 606.8 nm may be associated with chlorophyll *b* or xanthophylls (Ford 2000), whereas 671.6 nm with chlorophyll *a*. Note that both F_1 and F_2 identified 671.6 nm as a key wavelength. Finally, the wavelength of 978.6 nm was ascribed to C–H 3rd and 4th overtone, which was close to the wavelength of 980 nm indicated as principal absorption band of dry starch (Williams and Norris 1987).

Conclusion

Using Vis/NIR hyperspectral imaging and a PCA/FDA statistical approach, maize kernels artificially inoculated with different concentrations of AFB_1 could be differentiated from those that were not inoculated. Moreover, it is possible to discriminate between different levels of AFB_1 on the surface of maize kernels. Detection of AFB_1 artificially inoculated on kernel surfaces was possible at concentrations as low as 10 ppb. In addition, analysis of β coefficient curves of the 1st 2 discriminant factors produced by the FDA enabled the identification of several key wavelengths in the discriminative model. These results were consistent with the findings of several previous imaging/spectral studies on this area and demonstrated the potential for using Vis/NIR hyperspectral imaging along with a PCA/FDA statistical approach to identify and delineate the presence and level of AFB_1 on maize kernels.

However, this research was designed as a laboratory-based feasibility study using controlled samples in a controlled environment. To detect naturally occurring AFB_1 in maize kernels without any lab pre-treatment, multiple stages of work is needed to translate the findings of this work to a practical application. For example, in order to more accurately assess the exact concentration of AFB_1, the whole kernel rather than the residual staining of the AFB_1 should be selected as the ROIs to be analyzed. Also, different varieties of maize grown in different regions should be tested. Furthermore, since moisture levels are generally critical to prevent fungi growth, maize kernels with different gradients of moisture content should also be tested in order to build a more universal discriminant model.

Acknowledgments

The authors would like to thank Dr. Kurt C. Lawrence, Research Leader of Quality and Safety Assessment Research Unit, USDA, ARS, and Dr. Charles W. Bacon, Research Leader of the Toxicology and Mycotoxin Research Unit, USDA, ARS, for their guidance with the experimental design and providing samples. Mr. Vernon Savage, Engineering Technician with the Quality & Safety Assessment Research Unit, USDA, ARS, for his assistance in fabricating the Teflon holder and sealed acrylic box. The authors would also like to thank Dr. Jia-Sheng Wang, Professor, Dept. of Environmental Health Science College of Public Health, Univ. of Georgia, for his guidance on how to handle toxins. This work was supported financially by the China Natl. Science and Technology Support Program (2012BAK08B04).

Authors' Contributions

Wei Wang analyzed the data, selected the procedures and the algorithms to apply, and wrote the work. Gerald W. Heitschmidt cooperated to do the experiment, preprocessed the data, edited, and revised the paper. Prof. William R. Windham contributed to the discussion of experiment set up and evaluation of number of samples needed. Ms. Peggy Feldner undertook the preparation of AFB_1 solution and maize kernel samples. Dr. Xinzhi Ni evaluated the results and helped to revise the paper. Miss Xuan Chu assisted in the ROIs selection.

References

Abbas HK, Cartwright RD, Xie W, Shier WT. 2006. Aflatoxin and fumonisin contamination of maize (maize, Zea mays) hybrids in Arkansas. Crop Prot 25:1–9.
Berardo N, Pisacane V, Battilani P, Scandolara A, Pietri A, Marocco A. 2005. Rapid detection of kernel rots and mycotoxins in maize by near-infrared reflectance spectroscopy. J Agric Food Chem 53(21):8128–34.
Borman AM, Linton CJ, Miles SJ, Johnson EM. 2008. Molecular identification of pathogenic fungi. J Antimicrob Chemoth 61:7–12.
Castellano M, Ruiz-Filippi G, Gonza´ lez W, Roca E, Lema JM. 2007. Selection of variables using factorial discriminant analysis for the state identification of an anaerobic UASB–UAF hybrid pilot plant, fed with winery effluents. Water Sci Technol 56(2): 139–45.
Christensen D, Allesø M, Rosenkrands I, Rantanen J, Foged C, Agger EM, Andersen P, Nielsen HM. 2008. NIR transmission spectroscopy for rapid determination of lipid and lyoprotector content in liposomal vaccine adjuvant system CAF01. Eur J Pharm Biopharm 70(3):914–20.
Del Fiore A, Reverberi M, Ricelli A, Pinzari F, Serranti S, Fabbri AA, Bonifazi G, Fanelli C. 2010. Early detection of toxigenic fungi on maize by hyperspectral imaging analysis. Int J food Microbiol 144(1):64–71.
Delwiche SR, Gaines CS. 2005. Wavelength selection for monochromatic and bichromatic sorting of *fusarium*-damaged wheat. Appl Eng Agric 21(4):681–8.
Delwiche SR, Kim MS. 2000. Hyperspectral imaging for detection of scab in wheat, Proc. SPIE 4203, Biological Quality and Precision Agriculture II, 13 (December 29, 2000). DOI:10.1117/12.411752.
Dowell FE, Ram MS, Seitz LM. 1999. Predicting scab, vomitoxin, and ergosterol in single wheat kernels using near-infrared spectroscopy. Cereal Chem 76(4):573–76.
Dowell FE, Pearson TC, Maghirang EB, Xie F, Wicklow DT. 2002. Reflectance and transmittance spectroscopy applied to detecting fumonisin in single corn kernels infected with *Fusarium verticillioides*. Cereal Chem 79:222–6.
Fernández-Ibañez V, Soldado A, Martínez-Fernández A, de la Roza-Delgado B. 2009. Application of near infrared spectroscopy for rapid detection of AFB1 in maize and barley as analytical quality assessment. Food Chem 113:629–34.
Ford RH. 2000. Inheritance of kernel color in corn: explanations & investigations. AM Biol Teach 62(3):181–8.
Gorran A, Farzaneh M, Shivazad M, Rezaeian M, Ghassempour A. 2013. Aflatoxin B1-reduction of *Aspergillus flavus* by three medicinal plants (Lamiaceae). Food Control 31(1):218–23.
Hammami M, Rouissi H, Salah N, Selmi H, Al-Otaibi M, Blecker C, Karoui R. 2010. Fluorescence spectroscopy coupled with factorial discriminant analysis technique to identify sheep milk from different feeding systems. Food Chem 122:1344–50.
Herzallah SM. 2009. Determination of aflatoxins in eggs, milk, meat and meat products using HPLC fluorescent and UV detectors. Food Chem 114(3):1141–6.
Ivorra E, Girón J, Sánchez AJ, Verdú S, Barat JM, Grau R. 2013. Detection of expired vacuum-packed smoked salmon based on PLS-DA method using hyperspectral images. J Food Eng 117: 342–9.
Intl. Agency for Research on Cancer. 2002. Some traditional herbal medicines, some mycotoxins, naphthalene and styrene. IARC monographs on the evaluation of carcinogenic risks to humans (Vol. 82). Lyon, France: World Health Organization, p 1–556
Karoui R, Hammami M, Rouissi H, Blecker C. 2011. Mid infrared and fluorescence spectroscopies coupled with factorial discriminant analysis technique to identify sheep milk from different feeding systems. Food Chem 127: 743–8.
Lauro NC, Verde R, Irpino A. 2007. Factorial discriminant analysis. In: Edwin D, Monique NF, editor. Symbolic data analysis and the SODAS software. Hoboken, NJ: John Wiley & Sons, Inc.
Lin WS, Yang CM, Kuo BJ. 2012. Classifying cultivars of rice (*Oryza sativa* L.) based on corrected canopy reflectance spectra data using the orthogonal projections to latent structures (O-PLS) method. Chemometr Intell Lab 115:25–36.
Manetta AC. 2011. Aflatoxins: Their Measure and Analysis, In: Irineo TP, editor. Aflatoxins-Detection, Measurement and Control. Rijeka, Croatia: InTech. p 93–94.
Manley M, McGoverin CM, Engelbrecht P, Geladi P, 2012. Influence of grain topography on near infrared hyperspectral images. Talanta 89:223–30.

McDanell R, McLean AEM, Hanley AB, Heaney RK, Fenwick GR. 1988. Chemical and biological properties of indole glucosinolates (glucobrassicins): a review. Food Chem Toxicol 26(1):59–70.
Pearson TC, Wicklow DT, Maghirang EB, Xie F, Dowell FE. 2001. Detecting aflatoxin in single corn kernels by transmittance and reflectance spectroscopy. T Asae 44(5):1247–54.
Peiris KHS, Pumphrey MO, Dowell FE. 2009. NIR absorbance characteristics of deoxynivalenol and of sound and *Fusarium*-damaged wheat kernels. J Near Infrared Spec 17:213–21.
Piermarini S, Volpe G, Micheli L, Moscone D, Palleschi G. 2009. An ELIME-array for detection of aflatoxin B1 in corn samples. Food Control 20(4):371–5.
Polder G, van der Heijden GWAM, Waalwijk C, Young IT. 2005. Detection of *Fusarium* in single wheat kernels using spectral Imaging. Seed Sci Technol 33:655–68.
Roger JM, Sablayrolles JM, Steyer JP, Bellon-Maurel V. 2002. Pattern analysis techniques to process fermentation curves: application to discrimination of enological alcoholic fermentations. Biotechnol Bioeng 79(7):804–15. DOI:10.1002/bit.10338
Samarajeewa U, Sen AC, Fernando SY, Ahmed EM, Wei CI. 1991. Inactivation of aflatoxin B1 in corn meal, copra meal and peanuts by chlorine gas treatment. Food Chem Toxicol 29(1):41–7.
Serranti S, Cesare D, Marini F, Bonifazi G. 2013. Classification of oat and goat kernels using NIR hyperspectral imaging. Talanta 103:276–84.
Shahin MA, Symons SJ. 2009. Design of a multispectral imaging system for detecting mildew damage on wheat kernels. The Canadian Society for Engineering in Agricultural, Food, Environmental, and Biological Systems. Paper No. CSBE09-701
Shahin MA, Symons SJ. 2011. Detection of *Fusarium* damaged kernels in Canada Western Red Spring wheat using visible/near-infrared hyperspectral imaging and principal component analysis. Comput Electron Agr 75:107–12.
Singh CB, Jayas DS, Paliwal J, White NDG. 2010. Detection of midge-damaged wheat kernels using short-wave near-infrared hyperspectral and digital colour imaging. Bioproc Biosyst Eng 105:380–7.
Singh CB, Jayas DS, Paliwal J, White NDG. 2012. Fungal damage detection in wheat using short-wave near-infrared hyperspectral and digital color imaging. Int J Food Prop 15:11–24.
Tripathi S, Mishra HN. 2009. A rapid FT-NIR method for estimation of AFB1 in red chili powder. Food Control 20:840–6.
Vitale R, Bevilacqua M, Bucci R, Magrì AD, Magrì AL, Marini F. 2013. A rapid and non-invasive method for authenticating the origin of pistachio samples by NIR spectroscopy and chemometrics. Chemometr Intell Lab 121:90–9.
Wang D, Dowell FE, Ram MS, Schapaugh WT. 2004. Classification of fungal-damaged soybean seeds using near-infrared spectroscopy. Int J Food Prop 7(1):75–82.
Wang W, Heitschmidt, GW, Ni, X, Windham, WR, Hawkins, S, Chu, X. 2014. Identification of aflatoxin B1 on maize kernels surface using hyperspectral imaging. Food Control 42:78–86.
Waśkiewicz A, Beszterda M, Goliński P. 2012. Occurrence of fumonisins in food—an interdisciplinary approach to the problem. Food Control 26(2):491–9.
Williams P, Norris K, editors. 1987. Near-Infrared technology in the agricultural and food industries. St. Paul, Minn.: American Assn. of Cereal Chemists, Inc. p 59–76.
Williams PJ, Geladi P, Britz TJ, Manley M. 2012. Investigation of fungal development in maize kernels using NIR hyperspectral imaging and multivariate data analysis. J Cereal Sci 55: 272–8.
Wright MS, Greene-McDowelle DM, Zeringue Jr. HJ, Bhatnagar D, Cleveland TE. 2000. Effects of volatile aldehydes from *Aspergillus*-resistant varieties of corn on *Aspergillus parasiticus* growth and aflatoxin biosynthesis. Toxicon 38(9):1215–23.
Xing J, Symons S, Shahin M, Hatcher D. 2010. Detection of sprout damage in Canada Western Red Spring wheat with multiple wavebands using visible/near-infrared hyperspectral imaging. Biosyst Eng 106:188–94.